# Evolutionary clonal trajectories in nodular lymphocyte-predominant Hodgkin lymphoma with high risk of transformation

**Lisa Paschold,[1] Edith Willscher,[1] Julia Bein,[2] Martine Vornanen,[3] Dennis A. Eichenauer,[4] Donjete Simnica,[1] Benjamin Thiele,[5] Claudia Wickenhauser,[6] Andreas Rosenwald,[7] Heinz-Wolfram Bernd,[8] Wolfram Klapper,[9] Alfred C. Feller,[8] German Ott,[10] Falko Fend,[11] Sylvia Hartmann[2,12] and Mascha Binder[1]**

[1]Department of Internal Medicine IV, Oncology/Hematology, Martin-Luther-University Halle-Wittenberg, Halle (Saale), Germany: [2]Dr. Senckenberg Institute of Pathology, Goethe University Hospital of Frankfurt am Main, Frankfurt am Main, Germany; [3]Department of Pathology, Tampere University Hospital and University of Tampere, Tampere, Finland; [4]University of Cologne, First Department of Internal Medicine, Center for Integrated Oncology Aachen Bonn Cologne Dusseldorf, Cologne, and German Hodgkin Study Group, University Hospital Cologne, Cologne, Germany; [5]Department of Hematology and Oncology, University Medical Center Hamburg-Eppendorf, Hamburg, Germany; [6]Institute of Pathology, Martin-Luther-University Halle-Wittenberg, Halle (Saale), Germany; [7]Institute of Pathology, University of Würzburg and Comprehensive Cancer Center (CCC) Mainfranken, Würzburg, Germany; [8]Hematopathology Lübeck, Lübeck, Germany; [9]Department of Pathology, Division of Hematopathology and Lymph Node Registry, Schleswig-Holstein Medical Center, Campus Kiel, Kiel, Germany; [10]Department of Clinical Pathology, Robert-Bosch-Krankenhaus and Dr Margarete Fischer-Bosch Institute of Clinical Pharmacology, Stuttgart, Germany; [11]Institute of Pathology, Eberhard Karls University Tübingen, Tübingen, Germany and [12]Reference and Consultation Center for Lymph Node and Lymphoma Pathology, Goethe University, Frankfurt am Main, Germany

 doi:10.3324/haematol.2021.278427

Received: January 22, 2021.

Accepted: March 24, 2021.

Pre-published: April 22, 2021.

Correspondence: *MASCHA BINDER* - Mascha.Binder@uk-halle.de

## Supplemental Information

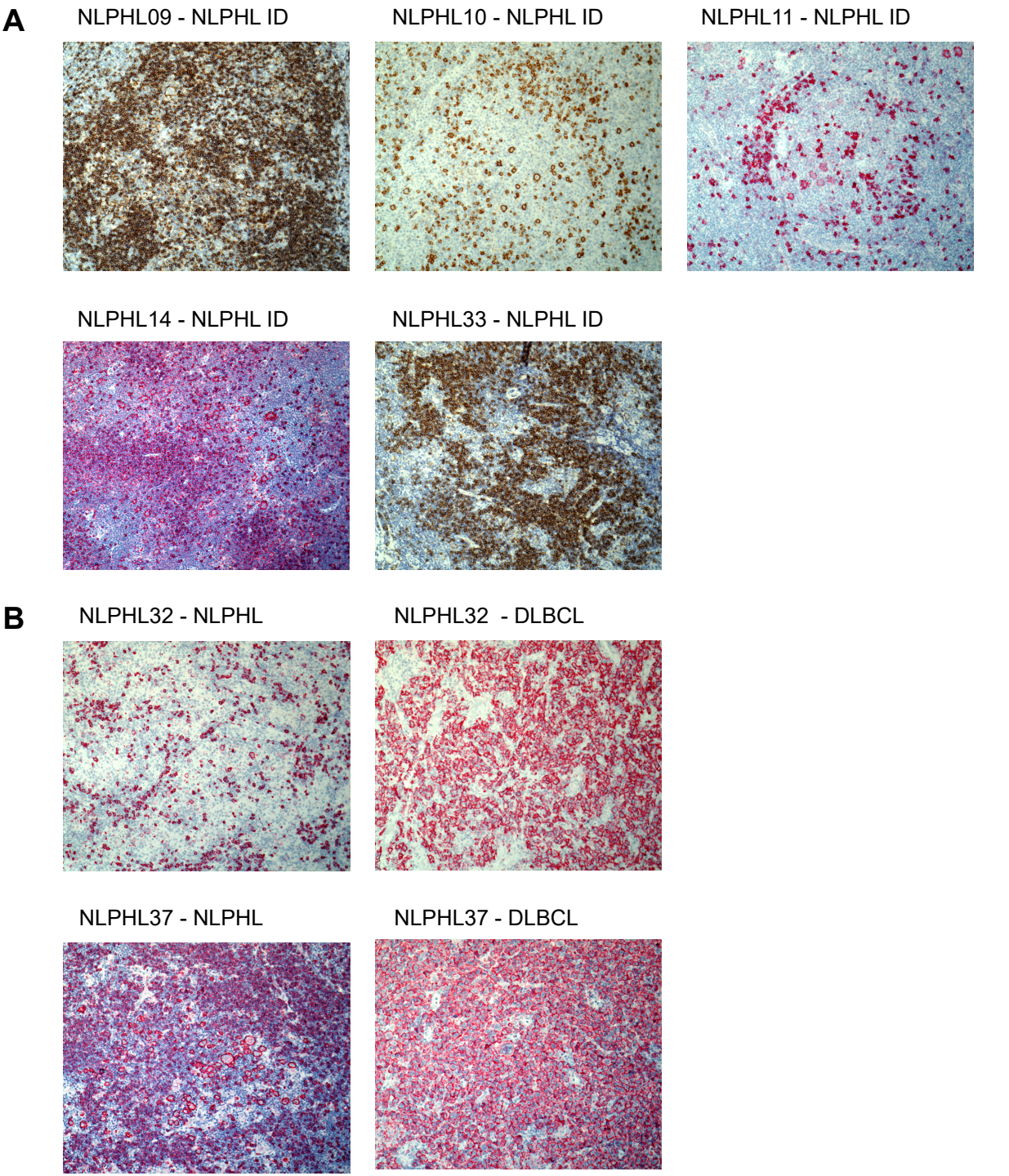


**Supplemental Figure 1: Histologic variant patterns of exemplary NLPHL cases.** Immunostaining with anti-CD20 antibody, 100x magnification. (**A)** NLPHL09, 10, 11, 14 and 33 at initial NLPHL diagnosis. (**B**) NLPHL32 and 37 with simultaneous involvement of the same lymph node by NLPHL and DLBCL.

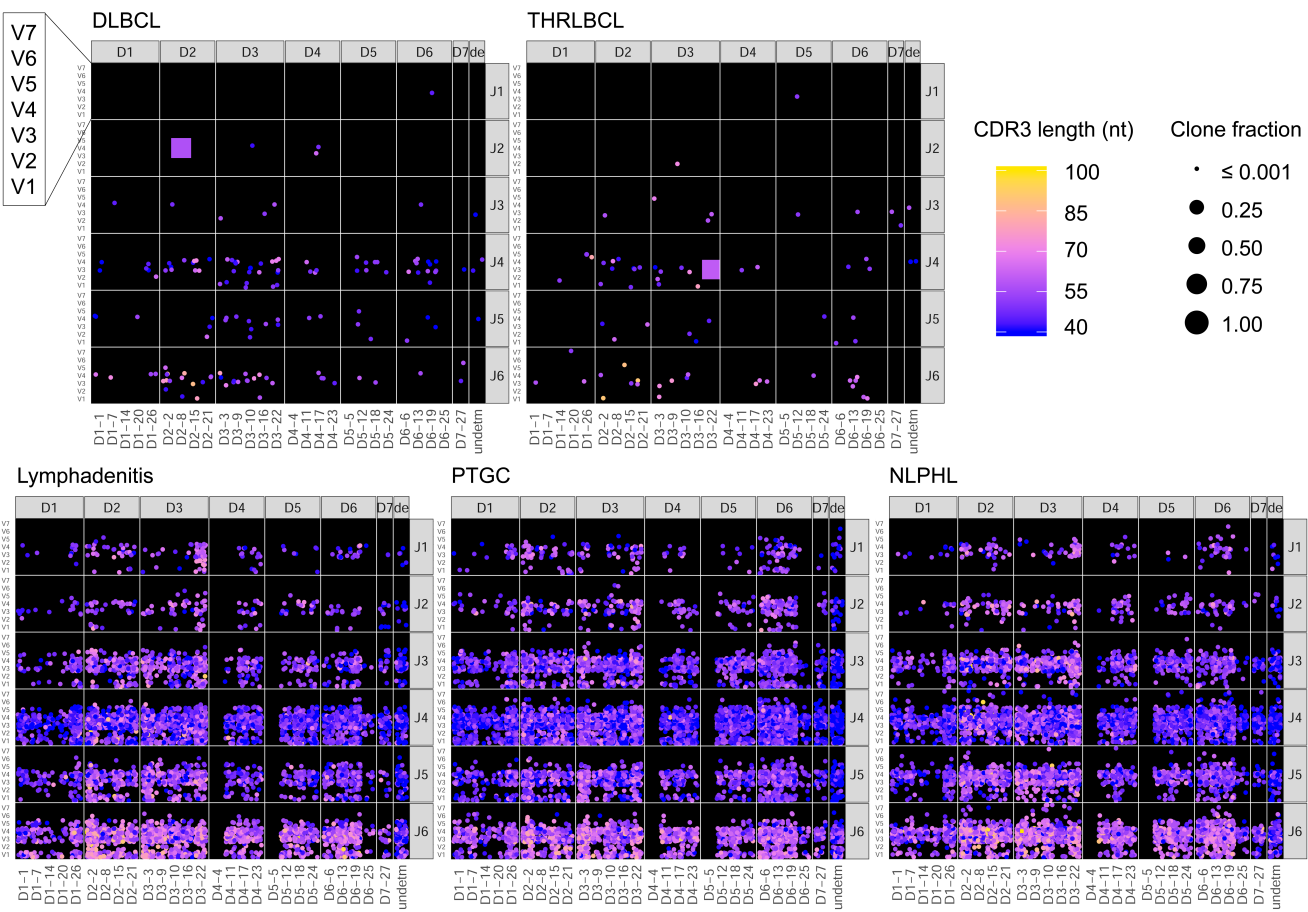


**Supplemental Figure 2: IGHV/D/J gene usage of B lineage repertoires from lymphoid tissue of NLPHL, PTGC, Lymphadenitis, DLBCL and THRLBCL.** Exemplary cases from each category are shown. Rearrangement of IGHV1-7 main groups and IGHJ1-6 are plotted on the vertical axis. IGHD subgroups are plotted on the horizontal axis. Each dot represents one immunoglobulin rearrangement colored according to its CDR3 length and sized according to clonal fraction. A square represents the malignant clone's IGHV/D/J rearrangement.

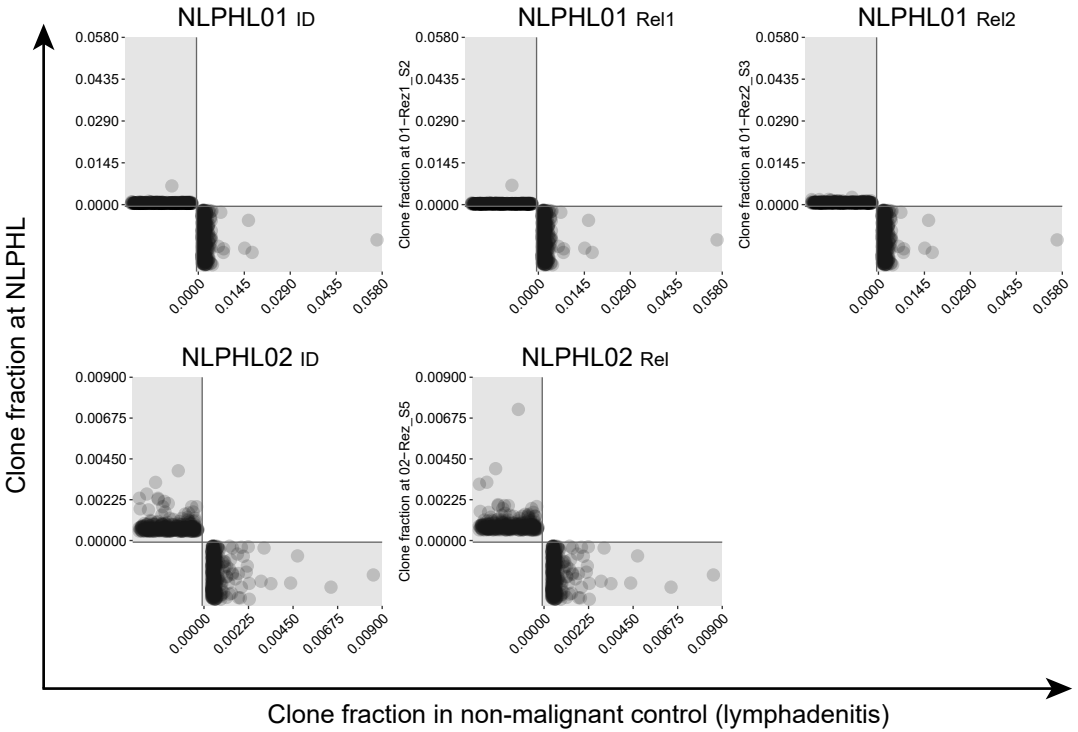


**Supplemental Figure 3: B lineage repertoire overlaps of two NLPHL cases with paired samples and corresponding benign lymphadenitis controls.** ID = initial diagnosis. Rel = relapse.

**Supplemental Table 1: Clinical characteristics of patients of cohorts 1-3.** ID = initial diagnosis, Rel =relapse.

| Patient-ID | Cohort | Timepoint | Disease stage | Age | Sex | IgD-Status | NLPHL variant pattern | DLBCL subtype | Follow up time/Years after ID | malignant clone type |
|---|---|---|---|---|---|---|---|---|---|---|
| NLPHL-07 | cohort 1 | single | NLPHL | 10 | male | positive | A | NA | 16 | NA |
| NLPHL-39 | cohort 1 | single | NLPHL | 17 | male | negative | E | NA | 6 | NA |
| NLPHL-43 | cohort 1 | single | NLPHL | 29 | male | negative | A | NA | 20 | NA |
| NLPHL-44 | cohort 1 | single | NLPHL | 11 | male | negative | A | NA | 19 | NA |
| NLPHL-45 | cohort 1 | single | NLPHL | 56 | male | positive | A | NA | 17 | NA |
| NLPHL-01 | cohort 2 | ID | NLPHL | 13 | male | positive | C | NA | NA | longCDR3 |
| NLPHL-01 | cohort 2 | Rel1 | NLPHL | 14 | male | positive | C | NA | 1 | longCDR3 |
| NLPHL-01 | cohort 2 | Rel2 | NLPHL | 16 | male | positive | C | NA | 3 | longCDR3 |
| NLPHL-02 | cohort 2 | ID | NLPHL | 15 | male | positive | C | NA | NA | longCDR3 |
| NLPHL-02 | cohort 2 | Rel | NLPHL | 16 | male | positive | C | NA | 1 | longCDR3 |
| NLPHL-03 | cohort 2 | ID | NLPHL | 23 | male | negative | A | NA | NA | longCDR3 |
| NLPHL-03 | cohort 2 | Rel | NLPHL | 27 | male | negative | A | NA | 4 | longCDR3 |
| NLPHL-04 | cohort 2 | ID | NLPHL | 14 | female | positive | A | NA | NA | longCDR3 |
| NLPHL-04 | cohort 2 | Rel | NLPHL | 15 | female | positive | A | NA | 1 | longCDR3 |
| NLPHL-09 | cohort 2 | ID | NLPHL | 51 | female | negative | A | NA | NA | longCDR3 |
| NLPHL-09 | cohort 2 | Rel | NLPHL | 52 | female | negative | A | NA | 1 | longCDR3 |
| NLPHL-12 | cohort 2 | ID | NLPHL | 27 | male | negative | C | NA | NA | NA |
| NLPHL-12 | cohort 2 | Rel | NLPHL | 37 | male | negative | A | NA | 10 | NA |
| NLPHL-13 | cohort 2 | ID | NLPHL | 59 | female | negative | A | NA | NA | no_longCDR3 |
| NLPHL-13 | cohort 2 | Rel | NLPHL | 76 | female | negative | A | NA | 17 | no_longCDR3 |
| NLPHL-14 | cohort 2 | ID | NLPHL | 14 | male | positive | C | NA | NA | longCDR3 |
| NLPHL-14 | cohort 2 | Rel | NLPHL | 14 | male | positive | C | NA | <1 | longCDR3 |
| NLPHL-15 | cohort 2 | ID | NLPHL | 30 | female | negative | A | NA | NA | no_longCDR3 |
| NLPHL-15 | cohort 2 | Rel | NLPHL | 32 | female | negative | A | NA | 2 | no_longCDR3 |
| NLPHL-16 | cohort 2 | ID | NLPHL | 24 | male | negative | A | NA | NA | no_longCDR3 |
| NLPHL-16 | cohort 2 | Rel | NLPHL | 27 | male | negative | E | NA | 3 | no_longCDR3 |
| NLPHL-17 | cohort 2 | ID | NLPHL | 40 | nd | negative | D/A | NA | NA | NA |
| NLPHL-17 | cohort 2 | Rel | NLPHL | 49 | nd | negative | A | NA | 9 | NA |
| NLPHL-18 | cohort 2 | ID | NLPHL | 49 | nd | negative | D/A | NA | NA | NA |
| NLPHL-18 | cohort 2 | Rel | NLPHL | 52 | nd | negative | A | NA | 3 | NA |
| NLPHL-20 | cohort 2 | ID | NLPHL | 29 | male | negative | A | NA | NA | no_longCDR3 |
| NLPHL-20 | cohort 2 | Rel | NLPHL | 44 | male | negative | A | NA | 15 | no_longCDR3 |

| | | | | | | | | | | |
|---|---|---|---|---|---|---|---|---|---|---|
| NLPHL-28 | cohort 2 | ID | NLPHL | 12 | male | positive | nd | NA | NA | longCDR3 |
| NLPHL-28 | cohort 2 | Rel | NLPHL | 13 | male | positive | nd | NA | 1 | longCDR3 |
| NLPHL-38 | cohort 2 | ID | NLPHL | 17 | female | negative | A | NA | NA | NA |
| NLPHL-38 | cohort 2 | Rel | NLPHL | 18 | female | negative | A | NA | 1 | NA |
| NLPHL-40 | cohort 2 | ID | NLPHL | 58 | female | negative | A/C | NA | NA | NA |
| NLPHL-40 | cohort 2 | Rel | NLPHL | 63 | female | negative | A | NA | 5 | NA |
| NLPHL-10 | cohort 3 | ID | NLPHL | 40 | male | negative | C/D | NA | NA | identical |
| NLPHL-10 | cohort 3 | Trafo | DLBCL | 41 | male | negative | NA | non-GCB | 1 | identical |
| NLPHL-11 | cohort 3 | ID | NLPHL | 33 | male | negative | C/D/E | NA | NA | identical |
| NLPHL-11 | cohort 3 | Trafo | DLBCL | 34 | male | negative | NA | non-GCB | 1 | identical |
| NLPHL-30 | cohort 3 | ID | NLPHL | 72 | female | negative | A/D | NA | NA | NA |
| NLPHL-30 | cohort 3 | Trafo | DLBCL | 80 | female | negative | NA | non-GCB | 8 | NA |
| NLPHL-31 | cohort 3 | ID | NLPHL | 50 | male | positive | A/E | NA | NA | NA |
| NLPHL-31 | cohort 3 | Trafo | DLBCL | 58 | male | positive | NA | non-GCB | 8 | NA |
| NLPHL-32 | cohort 3 | ID | NLPHL | 78 | male | negative | C | NA | NA | identical |
| NLPHL-32 | cohort 3 | Trafo | DLBCL | 78 | male | negative | NA | GCB | 0 (simultaneous) | identical |
| NLPHL-33 | cohort 3 | ID | NLPHL | 71 | male | negative | A | NA | NA | different |
| NLPHL-33 | cohort 3 | Trafo | DLBCL | 90 | male | negative | NA | GCB | 19 | different |
| NLPHL-34 | cohort 3 | ID | NLPHL | 70 | male | negative | D | NA | NA | different |
| NLPHL-34 | cohort 3 | Trafo | DLBCL | 85 | male | negative | NA | non-GCB | 15 | different |
| NLPHL-35 | cohort 3 | ID | NLPHL | 50 | male | negative | A/D | NA | NA | identical |
| NLPHL-35 | cohort 3 | Trafo | DLBCL | 67 | male | negative | NA | GCB | 17 | identical |
| NLPHL-37 | cohort 3 | ID | NLPHL | 51 | male | negative | A | NA | NA | NA |
| NLPHL-37 | cohort 3 | Trafo | DLBCL | 51 | male | negative | NA | non-GCB | 0 (simultaneous) | NA |
| NLPHL-41 | cohort 3 | ID | NLPHL | 35 | male | negative | nd | NA | NA | different |
| NLPHL-41 | cohort 3 | Trafo | DLBCL | 44 | male | negative | NA | nd | 9 | different |

# Methods

## *Amplification of IGH repertoire for next-generation sequencing (NGS)*

Genomic DNA of whole lymphoid tissue was isolated using the Maxwell® RSC FFPE Plus DNA Kit (Promega, Mannheim, Germany) according to the manufacturer's instructions. As described in (1-6), two consecutive PCR reactions were performed. The rearranged IGH locus was amplified in a multiplex PCR using 250 ng of genomic DNA and BIOMED2-FR1 or -FR3 primer pools.(7) In a second PCR, IGH fragments were tagged with Illumina-compatible adapters and 7 nucleotide barcodes. Most effective B lineage repertoire amplifications could be achieved by using primer pools annealing in FR3, while FR1 PCRs only sporadically resulted in successful amplification of the IGH locus. Phusion HS II was used for PCR amplification (Thermo Fisher Scientific Inc., Darmstadt, Germany). All primers were purchased from Metabion International AG (Martinsried, Germany). After electrophoretic separation on agarose gels, IGH amplicons were purified using the NucleoSpin® Gel and PCR Clean-up kit (Macherey-Nagel, Düren, Germany). Qubit platform (QIAGEN, Hilden, Germany) was used for quantification and samples were pooled to a final concentration of 4 nM. The IGH amplicon pools were analyzed for purity on an Agilent 2100 Bioanalyzer (Agilent Technologies, Böblingen, Germany) before being subjected to NGS.

## *Illumina NGS and data analysis*

NGS and demultiplexing was performed on an Illumina MiSeq sequencer (601-cycle single indexed, paired-end run, V3-chemistry). The rearranged IGH locus was analyzed using the MiXCR framework.(8) The IMGT library was used as reference for sequence alignment.(9) Sequences with less than 2 read counts were dropped. Only productive reads were used and all repertoires were normalized to 20,000 reads. All analyses and data plottings were performed using RStudio version 3.5.1. and the tcR(10), ade4(11), ggplot2(12) and tidyverse(13) packages.

Using FR3 PCRs, the CDR3 sequence as well as the IGHD- and IGHJ-gene segments could be reliably identified, while the alignment of the IGHV-gene segment was less robust due to the small size of the amplified segment. To account for this inaccuracy, we decided to indicate only the IGHV1-7 families, but not the individual IGHV-genes.

### *Immune repertoire metrics*

We calculated the clonality of the sequenced IGH repertoires according to the formula “1- Pielou's evenness.(14) In our setting, evenness measures the relative abundance of unique B cell clones in the repertoire and is calculated according to the formula J = H'/log2(S) with H' being the Shannon diversity(15) index and S the total clone number in a distinct sample.(16) A clonality index of 1 indicates that the analyzed sample contains only one clone whereas 0 indicates complete clonal diversity. The number of unique amino acid clonotypes is defined as richness. Shannon diversity index and principal component analysis were computed using RStudio version 3.5.1. and the tcR(10) package. Plotting was performed with GraphPad Prism 8.0.2 (GraphPad Software, La Jolla, CA, USA).

### *Identification of malignant LP or NHL IGH rearrangements*

For each patient, the top 300 clones per IGH repertoire were searched for identical CDR3 nucleotide sequences and identical IGHV/D/J genes in corresponding repertoire(s) of the same patient. In cases without overlap, the top 10 clones of each repertoire were searched for clones with identical IGHV/D/J genes and CDR3 nucleotide sequences with a Levenshtein distance of <10 to account for ongoing mutation. Matches obtained this way were bioinformatically fused to a single clone by summing up individual frequencies to be plotted in overlap dot plots. In addition, very dominant clones making up >10% of the repertoire were defined as malignant clones.

### *Visualization of LP/NHL subclonal evolutionary trajectories*

To identify clones related to the malignant LP or NHL rearrangement, all repertoires of the same patient were combined and subjected to approximately maximum-likelihood clustering using FastTreeMP(17). To exclude that sequences randomly sharing the same IGH rearrangement without belonging to the malignant clone were erroneously counted as clonally related, we spiked all tree analyses with an additional repertoire from non-malignant lymphadenitis as unspecific control to facilitate correct LP/NHL clustering based on CDR3 nucleotide sequence. Sequences in direct neighborhood to the malignant clone were counted as LP/NHL subclones if they shared the same IGHV/D/J rearrangement and a CDR3 nucleotide sequence with a Levenshtein distance of <10. LP/NHL subclones were visualized for each repertoire using the R package bubbles(18). The area size of the bubbles reflects the relative clone fraction of the LP/NHL subclones, with the summed fraction of the

subclones normalized to 1 for each repertoire. Evolution patterns were deduced from analysis of differences in somatic hypermutation between LP/NHL subclones.

## *References*


1. Schliffke S, Akyüz N, Ford CT, Mährle T, Thenhausen T, Krohn-Grimberghe A, Knop S, Bokemeyer C, Binder M. Clinical response to ibrutinib is accompanied by normalization of the T-cell environment in CLL-related autoimmune cytopenia. Leukemia. 2016 Nov;30(11):2232-2234. eng. Epub 2016/11/03. doi:10.1038/leu.2016.157. Cited in: Pubmed; PMID 27220665.

2. Schliffke S, Sivina M, Kim E, von Wenserski L, Thiele B, Akyüz N, Falker-Gieske C, Statovci D, Oberle A, Thenhausen T, Krohn-Grimberghe A, Bokemeyer C, Jain N, Estrov Z, Ferrajoli A, Wierda W, Keating M, Burger JA, Binder M. Dynamic changes of the normal B lymphocyte repertoire in CLL in response to ibrutinib or FCR chemo-immunotherapy. Oncoimmunology. 2018;7(4):e1417720. eng. Epub 2018/04/11. doi:10.1080/2162402x.2017.1417720. Cited in: Pubmed; PMID 29632735.

3. Akyüz N, Brandt A, Stein A, Schliffke S, Mährle T, Quidde J, Goekkurt E, Loges S, Haalck T, Ford CT, Asemissen AM, Thiele B, Radloff J, Thenhausen T, Krohn-Grimberghe A, Bokemeyer C, Binder M. T-cell diversification reflects antigen selection in the blood of patients on immune checkpoint inhibition and may be exploited as liquid biopsy biomarker. Int J Cancer. 2017 Jun 1;140(11):2535-2544. eng. Epub 2016/12/08. doi:10.1002/ijc.30549. Cited in: Pubmed; PMID 27925177.

4. Oberle A, Brandt A, Voigtlaender M, Thiele B, Radloff J, Schulenkorf A, Alawi M, Akyüz N, März M, Ford CT, Krohn-Grimberghe A, Binder M. Monitoring multiple myeloma by next-generation sequencing of V(D)J rearrangements from circulating myeloma cells and cell-free myeloma DNA. Haematologica. 2017 Jun;102(6):1105-1111. eng. Epub 2017/02/12. doi:10.3324/haematol.2016.161414. Cited in: Pubmed; PMID 28183851.

5. Mährle T, Akyüz N, Fuchs P, Bonzanni N, Simnica D, Germing U, Asemissen AM, Jann JC, Nolte F, Hofmann WK, Nowak D, Binder M. Deep sequencing of bone marrow microenvironments of patients with del(5q) myelodysplastic syndrome reveals imprints of antigenic selection as well as generation of novel T-cell clusters as a response pattern to lenalidomide. Haematologica. 2019 Jul;104(7):1355-1364. eng. Epub 2019/01/19. doi:10.3324/haematol.2018.208223. Cited in: Pubmed; PMID 30655375.

6. Schultheiss C, Paschold L, Simnica D, Mohme M, Willscher E, von Wenserski L, Scholz R, Wieters I, Dahlke C, Tolosa E, Sedding DG, Ciesek S, Addo M, Binder M. Next-Generation Sequencing of T and B Cell Receptor Repertoires from COVID-19 Patients Showed Signatures Associated with Severity of Disease. Immunity. 2020 Aug 18;53(2):442-455 e4. Epub 2020/07/16. doi:10.1016/j.immuni.2020.06.024. Cited in: Pubmed; PMID 32668194.

7. Brüggemann M, Kotrová M, Knecht H, Bartram J, Boudjogrha M, Bystry V, Fazio G, Froňková E, Giraud M, Grioni A, Hancock J, Herrmann D, Jiménez C, Krejci A, Moppett J, Reigl T, Salson M, Scheijen B, Schwarz M, Songia S, Svaton M, van Dongen JJM, Villarese P, Wakeman S, Wright G, Cazzaniga G, Davi F, García-Sanz R, Gonzalez D, Groenen PJTA, Hummel M, Macintyre EA, Stamatopoulos K, Pott C, Trka J, Darzentas N, Langerak AW, on behalf of the EuroClonality NGSwg. Standardized next-generation sequencing of immunoglobulin and T-cell receptor gene recombinations for MRD marker identification in acute lymphoblastic leukaemia; a EuroClonality-NGS validation study. Leukemia. 2019 2019/09/01;33(9):2241-2253. doi:10.1038/s41375-019-0496-7.

8. Bolotin DA, Poslavsky S, Mitrophanov I, Shugay M, Mamedov IZ, Putintseva EV, Chudakov DM. MiXCR: software for comprehensive adaptive immunity profiling. Nature Methods. 2015 2015/05/01;12(5):380-381. doi:10.1038/nmeth.3364.

9. Giudicelli V, Chaume D, Lefranc M-P. IMGT/GENE-DB: a comprehensive database for human and mouse immunoglobulin and T cell receptor genes. Nucleic Acids Research. 2005;33(suppl_1):D256-D261. doi:10.1093/nar/gki010.

10. Nazarov VI, Pogorelyy MV, Komech EA, Zvyagin IV, Bolotin DA, Shugay M, Chudakov DM, Lebedev YB, Mamedov IZ. tcR: an R package for T cell receptor repertoire advanced data analysis. BMC Bioinformatics. 2015 2015/05/28;16(1):175. doi:10.1186/s12859-015-0613-1.

11. Dray S, Dufour A-B. The ade4 Package: Implementing the Duality Diagram for Ecologists. 2007. 2007 2007-09-30;22(4):20. Epub 2007-09-02. doi:10.18637/jss.v022.i04.

12. Wickham H. ggplot2: Elegant Graphics for Data Analysis. Springer-Verlag New York; 2016. p. https://ggplot2.tidyverse.org.

13. Wickham H, Averick M, Bryan J, Chang W, McGowan L, François R, Grolemund G, Hayes A, Henry L, Hester J, Kuhn M, Pedersen T, Miller E, Bache S, Müller K, Ooms J, Robinson D, Seidel D, Spinu V, Takahashi K, Vaughan D, Wilke C, Woo K, Yutani H. Welcome to the Tidyverse. J of Open Source Softw. 2019;4(43). doi:10.21105/joss.01686.

14. Kirsch I, Vignali M, Robins H. T-cell receptor profiling in cancer. Mol Oncol. 2015 Dec;9(10):2063-70. eng. Epub 2015/09/26. doi:10.1016/j.molonc.2015.09.003. Cited in: Pubmed; PMID 26404496.

15. Shannon CE. A Mathematical Theory of Communication. Bell System Technical Journal. 1948;27(3):379-423. doi:10.1002/j.1538-7305.1948.tb01338.x.

16. Pielou EC. Species-diversity and pattern-diversity in the study of ecological succession. J Theor Biol. 1966 Feb;10(2):370-83. eng. Epub 1966/02/01. doi:10.1016/0022-5193(66)90133-0. Cited in: Pubmed; PMID 5964400.

17. Price MN, Dehal PS, Arkin AP. FastTree 2--approximately maximum-likelihood trees for large alignments. PLoS One. 2010 Mar 10;5(3):e9490. Epub 2010/03/13. doi:10.1371/journal.pone.0009490. Cited in: Pubmed; PMID 20224823.

18. Cheng J, Bostock M, Heer J. bubbles: d3 Bubble Chart htmlwidget. R package version 0.2.